

BROWN-HET-1001

September 1995

FORMATION OF HIGH REDSHIFT OBJECTS IN A COSMIC STRING THEORY WITH HOT DARK MATTER

R. MOESSNER^{1,2,a)} AND R. BRANDENBERGER^{1,3,b)}

1) *Brown University, Department of Physics*
Providence, RI 02912, USA

2) *Max Planck Institut für Astrophysik*
D-85740 Garching, Germany

3) *Physics Department, University of British Columbia*
Vancouver, B.C. V6T 1Z1, Canada

ABSTRACT

Using a modification of the Zel'dovich approximation adapted to hot dark matter, the accretion of such matter onto moving cosmic string loops is studied. It is shown that a large number of $10^{12}M_{\odot}$ nonlinear objects will be produced by a redshift of $z = 4$. These objects could be the hosts of high redshift quasars.

a) email: moessner@het.brown.edu

b) email: rhb@het.brown.edu

1. Introduction

Observation of high redshift objects has emerged as a powerful tool for testing theories of structure formation. For example, in inflationary Universe models, the epoch when the first massive nonlinear structures (which could be the hosts of quasars or primordial galaxies) form is a sensitive function of the fraction of hot dark matter. Recent data on the abundance of damped Lyman alpha absorption systems (DLAS)¹⁾ and on the quasar abundance²⁾ has provided tight constraints on inflation-based models of structure formation with adiabatic density fluctuations and mixed dark matter.

Searches for high redshift quasars have been going on for some time²⁾. The quasar luminosity function is observed to rise sharply as a function of redshift z until $z \simeq 2.5$. According to recent results from the Palomar grism survey by Schmidt et al. (1995)²⁾, it peaks in the redshift interval $z \in [1.7, 2.7]$ and declines at higher redshifts. Irwin et al.²⁾ on the other hand find that the luminosity function is constant up to redshifts of about 4. Quasars (QSO) are extremely luminous, and it is generally assumed that they are powered by accretion onto black holes. It is possible to estimate the mass of the host galaxy of the quasar as a function of its luminosity, assuming that the quasar luminosity corresponds to the Eddington luminosity of the black hole. For a quasar of absolute blue magnitude $M_B = -26$, the host galaxy mass can be estimated as³⁾

$$M_G = c_1 10^{12} M_\odot, \tag{1.1}$$

where c_1 is a constant which contains the uncertainties in relating blue magnitude to bolometric magnitude of quasars, in the baryon fraction of the Universe and in the fraction of baryons in the host galaxy able to form the compact central object (taken to be 10^{-2}). The best estimate for c_1 is about 1. Models of structure formation have to pass the test of producing enough early objects of sufficiently large mass to host the observed quasars.

Damped Lyman alpha systems provide potentially even more powerful constraints on structure formation models. Evidence is mounting⁴⁾ that the absorption line systems observed in the spectrum of distant quasars are due to progenitors of typical galaxies. Based on the number density of absorption lines per frequency interval and on the column density calculated from individual absorption lines, the fraction of Ω in bound neutral gas (denoted by Ω_g) can be estimated. Recent observational results¹⁾ indicate that

$$\Omega_g(z) > 10^{-3} \tag{1.2}$$

for $z \in [1,3]$, with the highest value in fact taken on at $z = 3$! Note that the above corresponds to a value Ω in bound matter which is larger by a factor of f_b^{-1} , where f_b is the fraction of bound matter which is baryonic. In a $\Omega = 1$ cosmology, the value of f_b is expected to be of the order 10^{-1} .

The constraints coming from observation of high redshift objects for inflation-based models of structure formation were studied by several groups. In Ref. 7, it was shown that the high redshift quasar abundance is compatible with an unbiased cold dark matter (CDM) model^{c)}, but that the theory predicts an exponential decrease of the quasar abundance for $z > 5$. Recently⁸⁾, this analysis has been extended to mixed dark matter (MDM) models. The abundance of damped Lyman alpha systems was used in Refs. 3, 5 & 6 to further constrain MDM models. It was found that models with a fraction of hot dark matter (HDM) exceeding $\Omega_\nu = 0.2$ do not predict enough nonlinear structures at high redshift in order to be able to explain the data.

However, there exists a viable class of alternative theories of structure formation, the cosmic string (CS) models. In these models, density fluctuations are generated by topologically stable strings of trapped energy density (one-dimensional topological defects in a relativistic field theory describing matter), instead of originating as the result of quantum fluctuations during an early period of exponential

c) A model with flat spectrum ($n = 1$), $\Omega = 1$, and vanishing cosmological constant Λ .

expansion of the Universe. The main purpose of this paper is to present a preliminary study of the constraints on cosmic string models which can be derived using the QSO and DLAS abundances. The model we are most interested in is a cosmic string theory in a spatially flat ($\Omega = 1$) Universe with only HDM and baryons. This model is briefly reviewed in Section 2.

Our main result is that for reasonable values of the parameters of the model, the CS and HDM theory is compatible with the present observational constraints on the quasar abundance of the Palomar grism survey by Schmidt et al.²⁾, which are plotted in Figure 1. We will compare these observations for the comoving space density of quasars brighter than $M_B = -26$ with the abundance of objects of mass greater than M_G (given in (1.1)) in the cosmic string and hot dark matter model.. We also comment on the implications of the DLAS abundance (as given by (1.2)) for cosmic strings.

Our result is quite nontrivial. The reason why inflationary MDM models with a large fraction of HDM do not predict a sufficient abundance of nonlinear objects at high redshifts is that the spectrum of density perturbations is suppressed at small wavelengths (those which first become nonlinear in the standard CDM inflationary model) by neutrino free streaming⁹⁾. The primordial power spectrum in a cosmic string theory is scale invariant¹⁰⁾, as it is in inflation-based models. The reason why a CS and HDM model is viable at all is that cosmic strings survive free streaming¹¹⁾. Since the strings are long-lived seed perturbations (as opposed to adiabatic dark matter fluctuations), accretion of dark matter on small scales – wavelength $\lambda < \lambda_J^{max}$, where λ_J^{max} is the maximal neutrino free streaming scale (whose value is given later) – is delayed but not prevented. Thus, the spectrum of density perturbations is not exponentially cut off below λ_J^{max} as it is for an inflationary HDM theory. It is¹²⁾, however, suppressed by a power of λ/λ_J^{max} compared to that of an inflationary CDM model. It also has a smaller amplitude than the MDM model with $\Omega_\nu = 0.2$. Hence, it would seem that the CS and HDM model would be unable to explain the abundance of high redshift QSO and DLAS. However, as explained in the following paragraph, the above reasoning misses a

crucial point.

In the cosmic string theory – in contrast to inflation-based models – the density field is not a Gaussian random field. There are localized high density peaks even when the average density contrast is small. Hence, knowledge of the density power spectrum is insufficient to calculate the number density of nonlinear objects.

In particular, cosmic string loops seed large amplitude local density contrasts. In this paper, we study the accretion of hot dark matter onto moving string loops and use the results to compute the number density of high redshift objects as a function of a parameter ν which determines the number density of loops in the scaling solution (see Section 2). We demonstrate that for realistic values of ν , the number of massive nonlinear objects at redshifts ≤ 4 satisfies the recent observational constraint of quasar abundances (see Figure 1). We also comment on the implications of (1.2).

The next section of this paper contains a brief review of the CS and HDM theory of structure formation. In Section 3 we summarize the methods used: a Zel’dovich approximation¹³⁾ technique modified¹⁴⁾ to HDM and its adaptation to moving seed perturbations¹⁵⁾. Section 4 contains the main calculations, and in Section 5 we discuss the results. Units in which $\hbar = c = k_B = 1$ are used throughout, and a Hubble constant of $H = 50 h_{50} \text{kms}^{-1} \text{Mpc}^{-1}$ and a redshift at equal matter and radiation of $z_{eq} = 5750 \Omega h_{50}^2$ are used.

2. Brief Review of the Cosmic String and Hot Dark Matter Theory

Cosmic strings¹⁶⁾ are one-dimensional topological defects which are predicted in many relativistic field theories describing matter. In such theories, a network of strings forms during a phase transition in the very early Universe. These strings are characterized by a mass per unit length μ (which in principle is the only free parameter in a cosmic string model) which determines their gravitational effects.

After the time of formation, the network of strings rapidly approaches a “scaling solution”, a distribution of defects whose statistical properties are time independent when lengths are rescaled by dividing by the Hubble radius. The mean separation of the strings increases by having strings interconnect and chop off loops. The scaling solution of the string network is characterized by a fixed number N of long strings crossing each Hubble volume at any time t , and the presence of loops with a distribution

$$n(l, t) = \nu l^{-2} t^{-2}, \quad (2.1)$$

where l is the length of the loop and ν is a constant. The quantity $n(l, t)dt$ gives the number per unit physical volume at time t of loops with lengths in the interval between l and $l + dl$. The loops are remnants of string intercommutations at times $t' < t$. Loops oscillate and decay slowly by emitting gravitational radiation. Hence, there is a lower cutoff value of l for the distribution (2.1) given by

$$l_{min} \sim G\mu t, \quad (2.2)$$

G being Newton’s constant. Below l_{min} , the distribution $n(l, t)$ becomes constant. We shall not discuss this point since it will not be relevant to our computations.

In principle, the properties of the scaling solution and hence also the value of the constant ν is calculable, albeit only numerically. In practice, however, the dynamics of the defect network is quite complicated and the numerical resolution inadequate to solve this problem. Thus, we must treat ν as an undetermined constant. There are two more such constants which are denoted by α and β . The first constant determines the mean radius R_f of a string loop at the time of formation

$$R_f(t) = \alpha t, \quad (2.3)$$

the second relates the mean radius R to the length l of a loop:

$$l = \beta R. \quad (2.4)$$

Numerical simulations¹⁷⁾ indicate that $\alpha \leq 10^{-2}$ and $\beta \simeq 10$. They also indicate that $N \sim 10$. From these values it follows that – unless ν is extremely large – most of the mass of the string network resides in long strings (where long strings are defined operationally as strings which are not loops with radius smaller than the Hubble radius).

In the cosmic string theory there are two basic mechanisms which seed structures, loops and wakes. String loops act gravitationally almost like point mass objects when viewed from distances larger than R . Long straight strings, on the other hand, lead to planar over-dense regions called wakes¹⁸⁾. On distance scales smaller than its curvature radius, the local gravitational attraction of a string vanishes. However, space perpendicular to the string is conical with deficit angle $8\pi G\mu$. Hence, a string moving with transverse velocity v_s will impart a velocity perturbation

$$\delta v = 4\pi G\mu v_s \gamma(v_s) \quad (2.5)$$

towards the plane behind the string, where $\gamma(v)$ is the relativistic γ factor. This develops into a planar over-dense region behind the string, the wake.

Since most of the mass in the string network is in long strings, the wake mechanism will be responsible for the formation of most of the present structure in the Universe. The thickest and most numerous wakes are those created at the time of equal matter and radiation (t_{eq} ¹⁹⁾). The cosmic string theory hence predicts a distinguished scale and topology of the large-scale structure in encouraging agreement with the data from the CfA galaxy redshift survey²⁰⁾.

The scaling for the defect network leads to a scale invariant spectrum of density perturbations, which in turn leads to a “scale-invariant” ($n = 1$) spectrum of microwave anisotropies²¹⁾. Normalizing the model by the COBE results gives²²⁾

$$G\mu \simeq 10^{-6}. \quad (2.6)$$

The accretion of hot dark matter onto cosmic string wakes was considered in

detail in Ref. 14. It was found that the first comoving scale to go nonlinear about a wake caused by a string at time t_{eq} is

$$q_{max}(t_{eq}) = v_{eq} z_{eq} t_{eq} \simeq v_{eq} \cdot 50 h_{50}^{-2} \text{ Mpc} \quad (2.7)$$

where v_{eq} is the mean hot dark matter velocity at t_{eq} . In a $\Omega = 1$ Universe, v_{eq} is about 0.1. Hence, the distance q_{max} is in good agreement with the observed thickness of the CfA galaxy sheets²⁰).

Note, however, that the first dark matter nonlinearities about wakes form only at late times, at a redshift¹⁴⁾

$$z_{max} = \frac{24\pi}{5} G\mu v_s \gamma(v_s) v_{eq}^{-1} z_{eq}, \quad (2.8)$$

which for $v_s \gamma(v_s) \simeq 1$ and for the value of $G\mu$ from (2.6) corresponds to a redshift of about 1. Before this redshift, no nonlinearities form as a consequence of accretion onto a single uniform wake.

Thus, in the cosmic string and hot dark matter theory, a different mechanism is required in order to explain the origin of high redshift objects. Possible mechanisms related to wakes are early structure formation at the crossing sites of different wakes²³⁾, small-scale structure of the strings giving rise to wakes^{24,25,26)}, and inhomogeneities inside of wakes²⁶⁾. In this paper, however, we will explore a different mechanism, namely the accretion of hot dark matter onto loops.

In earlier work,¹¹⁾ the accretion of hot dark matter onto static cosmic string loops was studied. It was found that in spite of free streaming, the nonlinear structure seeded by a point mass grows from inside out, and that the first nonlinearities form early on (accretion onto string filaments proceeds similarly²⁵⁾). In the context of the “old” cosmic string scenario (wakes unimportant), this mechanism was used in Ref. 27 to derive the mass function of galaxies. Since loop accretion leads to nonlinear structures at high redshift, we will now investigate this mechanism in detail to see whether enough high redshift massive objects to satisfy the QSO constraints and (1.2) form.

3. Modified Zel'dovich Approximation

We will use the Zel'dovich approximation¹³⁾ and modifications thereof to study the accretion of hot dark matter onto moving string loops. The Zel'dovich approximation is a first order Lagrangian perturbation theory technique in which the time evolution of the comoving displacement ψ of a dark matter particle from the location of the seed perturbation is studied.

The physical distance of a dark matter particle from the center of the cosmic string loop is

$$h(q, t) = a(t)[q - \psi(q, t)]. \quad (3.1)$$

The scale factor $a(t)$ is normalized such that $a(t_0) = 1$, where t_0 is the present time. The Zel'dovich approximation is based on combining the Newtonian equation for h

$$\ddot{h} = -\nabla_h \Phi \quad (3.2)$$

with the Poisson equation for the Newtonian gravitational potential Φ and linearizing in ψ . For a pointlike seed mass of magnitude m located at the comoving position $\underline{q}' = 0$ the resulting equation is

$$\ddot{\psi} + 2\frac{\dot{a}}{a}\dot{\psi} + 3\frac{\ddot{a}}{a}\psi = \frac{Gm}{a^3 q^2}. \quad (3.3)$$

This equation describes how as a consequence of the seed mass, the motion of the dark matter particles away from the seed (driven by the expansion of the Universe) is gradually slowed down. If the seed perturbation is created at time t_i and the dark matter is cold, then the appropriate initial conditions for ψ are

$$\psi(q, t_i) = \dot{\psi}(q, t_i) = 0, \quad (3.4)$$

leading – for $a(t) \sim t^{2/3}$ appropriate in the matter dominated epoch $t > t_{eq}$ – to

the solution

$$\psi(q, t) = \frac{9}{10} Gm \left(\frac{t_0}{q} \right)^2 \left(\frac{t}{t_i} \right)^{2/3}. \quad (3.5)$$

As formulated above, the Zel'dovich approximation only works for cold dark matter, particles with negligible thermal velocities. The theory of interest to us, however, is based on hot dark matter. Luckily, the Zel'dovich approximation can be modified for HDM¹⁴⁾. HDM particles have large thermal velocities. At time t , the free streaming length in comoving coordinates is

$$\lambda_J(t) = v(t)z(t)t, \quad (3.6)$$

where $v(t) \sim z(t)$ is the hot dark matter velocity. The length $\lambda_J(t)$ is the mean distance an HDM particle will move in one expansion time. Free streaming erases density perturbations on scales $q < \lambda_J(t)$, a scale which decreases as $t^{-1/3}$ as t increases.

A simple prescription^{d)} for taking into account free streaming in the Zel'dovich approximation is to – for a fixed comoving scale q – only let the perturbation start to develop at time $t_s(q)$ when

$$\lambda_J(t_s(q)) = q, \quad (3.7)$$

i.e., replace the initial conditions (3.4) by

$$\psi(q, \tilde{t}_s(q)) = \dot{\psi}(q, \tilde{t}_s(q)) = 0 \quad (3.8)$$

with

$$\tilde{t}_s(q) = \max \{t_i, t_s(q)\}. \quad (3.9)$$

d) Note that this prescription has been shown¹⁴⁾ to give good agreement with an analysis obtained by tracking the full phase space distribution of HDM particles by means of the linearized collisionless Boltzmann equation.

The result for the comoving displacement $\psi(q)$ then becomes

$$\psi(q, t) = \frac{9}{10} Gm \left(\frac{t_0}{q} \right)^2 \left(\frac{t}{\tilde{t}_s(q)} \right)^{2/3}. \quad (3.10)$$

We can now define the mass that has gone nonlinear about a seed perturbation as the rest mass inside of the shell which is “turning around”, i.e. for which

$$\dot{h}(q, t) = 0. \quad (3.11)$$

This yields an equation

$$q = 2\psi(q, t) \quad (3.12)$$

for the scale $q_{nl}(t)$ which is turning around at time t . For cold dark matter, Eq. (3.5) can be combined with Eq. (3.12) to obtain $q_{nl}(t)$ as well as the corresponding mass

$$M_{CDM}(t) = \frac{2}{5} m \left(\frac{t}{t_i} \right)^{2/3}. \quad (3.13)$$

Note the similarity of this result to what can be obtained in linear perturbation theory: $(t/t_i)^{2/3}$ is precisely the growth factor of linear cosmological perturbations on small scales.

For HDM, Eqs. (3.8), (3.10) and (3.12) can be combined to yield

$$M_{HDM}(t) = \frac{8}{125} \frac{m^3}{M_{eq}^2} \left(\frac{t}{t_{eq}} \right)^2 \quad (3.14)$$

with

$$M_{eq} = \frac{2}{9} \frac{v_{eq}^3 t_{eq}}{G}. \quad (3.15)$$

A further complication is due to the finite velocity of the cosmic string loops. This implies that we must extend the Zel’dovich approximation technique to moving sources. For CDM, this was done by Bertschinger¹⁵⁾ with the interesting result

that there is to a first approximation no change in the total mass accreted. The suppression of the growth of perturbations in the direction perpendicular to the direction of motion of the seed mass is cancelled by the larger length of the non-linear region in the direction of motion. For HDM, however, there will be a net suppression of growth if the seed mass is moving. It will be important for us to take this effect into account.

Given a moving point source, the basic Zel'dovich approximation equation (3.3) becomes a vector equation

$$\ddot{\underline{\psi}} + 2\frac{\dot{a}}{a}\dot{\underline{\psi}} + 3\frac{\ddot{a}}{a}\underline{\psi} = \frac{Gm(\underline{q} - \underline{q}')}{a^3|\underline{q} - \underline{q}'|^3} \quad (3.16)$$

where $\underline{q}'(t)$ indicates the comoving position of the source. Without loss of generality we can take the source to move along the z axis with initial velocity v_i at time t_i , so that¹⁵⁾

$$\underline{q}'(t) = 3v_it_i \left(1 - \left(\frac{a(t)}{a(t_i)} \right)^{-1/2} \right) \underline{e}_z z(t_i), \quad (3.17)$$

\underline{e}_z being the unit vector along the z axis. In the matter dominated epoch Equation (3.16) can be solved exactly¹⁵⁾ (taking $q_y = 0$ without loss of generality)

$$\underline{\psi}(\underline{q}, t) = b(t)d_i[f_x(\underline{q}, t)\underline{e}_x + f_z(\underline{q}, t)\underline{e}_z] \quad (3.18)$$

with

$$\begin{aligned} d_i &= 3v_it_iz(t_i) \\ b(t) &= \frac{1}{15} \frac{Gm}{v_i^3 t_i} \frac{a(t)}{a(t_i)} \end{aligned} \quad (3.19)$$

and where f_x and f_z are known functions of \underline{q}, t and d_i which at late times become independent of time and contain the information about the geometry of the pattern of accretion onto the moving loop. In particular, the transverse displacement at

late times approaches

$$f_x(\underline{q}) = \left(\frac{d_i}{q_x}\right)^2 \left[\frac{q_x}{d_i^2} (R_\infty - R_i) + \frac{q_x q_z}{R_i d_i} \right] \equiv \frac{1}{2} \left(\frac{d_i}{q_x}\right)^2 k(\underline{q}). \quad (3.20)$$

In the above,

$$R(\underline{q}, t) = [q_x^2 + (q_z - q'_z(t))^2]^{1/2}, \quad (3.21)$$

$R_i = R(\underline{q}, t_i)$, $R_\infty = R(\underline{q}, t_\infty)$, and $k(\underline{q})$ is the factor by which the accretion at \underline{q} is suppressed due to the motion of the source.

It is easy to check that for $q^2 \gg d_i^2$ the factor $k(\underline{q})$ tends to 1 (for $q_x^2 \gg q_z^2$) and that the result for $\psi(q, t)$ from (3.18) goes to the result of (3.5). For rapidly moving loops we are interested in the opposite limit $d_i^2 \gg q^2$. In this case, evaluated at $q_z = 0$, the suppression factor becomes

$$k(q_x) \rightarrow 2 \frac{q_x}{d_i}. \quad (3.22)$$

In this case, the “turn-around” condition

$$q_x = 2\psi_x \quad (3.23)$$

for transverse accretion yields

$$q_x^2 \simeq \frac{18}{5} G m t_i \left(\frac{t_0}{d_i}\right) \left(\frac{t}{t_i}\right)^{2/3}. \quad (3.24)$$

For a cosmic string loop formed at time t_i whose mass is (see (2.3) and (2.4))

$$m = \alpha\beta\mu t_i \quad (3.25)$$

this gives

$$q_x(t_i, t) = \left(\frac{6}{5}\alpha\beta\right)^{1/2} (G\mu)^{1/2} v_i^{-1/2} t_0 z^{-1/2}(t). \quad (3.26)$$

From this result we can immediately recover Bertschinger’s result¹⁵⁾ that accretion of CDM onto a moving loop is not suppressed: the total accreted mass $M(t)$ is

proportional to

$$M(t) \sim q_x^2(t) d_i \rho_c \quad (3.27)$$

where ρ_c is the background comoving energy density. The factors of v_i evidently cancel!

We are interested in the accretion of HDM onto moving loops. Provided that the turn-around distance q_x of (3.26) exceeds the initial comoving free streaming distance, i.e.

$$q_x(t_i, t) > \lambda_J(t_i) \quad (3.28)$$

then the above analysis can also be applied to HDM. We will check this condition in our calculations in the following section.

4. Computations

At this point, we are able to use the methods described in the previous section to compute the number density $n_G(> M_1, t)$ in nonlinear objects heavier than M_1 , and the fraction Ω_{nl} of the critical density in such objects at high redshift $z(t)$ in the cosmic string and hot dark matter model. By considering only the accretion onto string loops we will be underestimating these quantities.

It can be shown²⁷⁾ that in an HDM model string loops accrete matter independently, at least before the large-scale structure turns nonlinear at the redshift given by (2.8) which is about 1, i.e., later than the times of interest in this paper. Hence, the number density $n(l, t)$ of loops of length l given by (2.1) can be combined with the mass $M(l)$ accreted by an individual loop (which follows from (3.13) and (3.14)) to give the mass function $n(M, t)$. Here, $n(M, t)dM$ is the number density of objects with mass in the interval between M and $M + dM$ at time t . This in

turn determines the comoving density in objects of mass $M > M_1$,

$$n_G(> M_1, t) = z^{-3}(t) \int_{M_1}^{M_2} dM n(M) \quad (4.1)$$

and the fraction of the critical density in objects of mass greater than M_1 , $\Omega_{nl}(t)$:

$$\Omega_{nl}(t) = 6\pi G t^2 \int_{M_1}^{M_2} dM M n(M). \quad (4.2)$$

If we want to compare with the observational results from QSO counts we must use appropriate integration limits M_1 and M_2 in (4.1) and (4.2). The mass M_1 is the mass limit corresponding to the limiting QSO luminosity of the observational sample given in (1.1), $M_1 = c_1 10^{12} M_\odot$. For comparison with damped Lyman alpha systems, the lower cut-off mass M_1 is somewhat smaller, but we will not need the exact value. For large loop radii, the approximation of treating the loop as a point mass breaks down. This will lead to a time dependent upper mass cutoff $M_2(t)$. A rough criterion for $M_2(t)$ can be obtained by demanding that the mass $M(t)$ accreted onto a loop exceed the mass in a sphere of radius equal to the loop radius at t_i ,

$$M(t) > \frac{1}{6\pi G t_i^2} \frac{4\pi}{3} (\alpha t_i)^3. \quad (4.3)$$

Using the CDM mass formula (3.13) with initial mass (3.25) yields the estimate

$$M_2(t) \simeq \frac{2}{5} \left(\frac{9}{5}\right)^{1/2} (\beta G \mu)^{3/2} \frac{t_0}{G} z(t)^{-3/2}. \quad (4.4)$$

Since

$$\frac{t_0}{G} \simeq 8 \cdot 10^{22} h_{50}^{-1} M_\odot, \quad (4.5)$$

the value of M_2 is much greater than both M_1 and the maximal neutrino Jeans mass $M'(t)$, the largest mass which is affected by free streaming. This justifies the use of the CDM mass formula (3.13).

As indicated above, there is another mass which is crucial for the computation of $n_G(t)$ and $\Omega_{nl}(t)$, namely $M'(t)$. The easiest way to determine $M'(t)$ is to ask for the value of M for which the mass formulas (3.13) and (3.14) intersect:

$$\frac{2}{5}m \left(\frac{t}{t_i}\right)^{2/3} = \left(\frac{2}{5}\right)^3 \frac{m^3}{M_{eq}^2} \left(\frac{t}{t_{eq}}\right)^2. \quad (4.6)$$

Using the expression (3.25) for m and taking account of (3.15), one finds

$$M'(t) = \frac{2}{5} \left(\frac{5}{9}\right)^{1/4} (\alpha\beta G\mu)^{3/4} v_{eq}^{3/4} z(t)^{-3/4} z_{eq}^{-3/4} \frac{t_0}{G}, \quad (4.7)$$

from which it indeed follows that – at least for the redshifts we are interested in – $M'(t)$ is smaller than $M_2(t)$.

As a self-consistency check we note that M_1 is larger than the mass accreted onto a loop created at t_{eq} . Hence, it is consistent to restrict our attention to the matter epoch $t > t_{eq}$.

Since the functional form of $M(m)$ and hence $M(l)$ changes at $M = M'$, the functional forms of the mass function $n(M)$ will be different above and below M' . Thus

$$n_G(> M_1, t) = z^{-3}(t) \left[\int_{M_1}^{M'(t)} dM n_H(M) + \int_{M'(t)}^{M_2(t)} dM n_C(M) \right]. \quad (4.8)$$

Similarly for $\Omega_{nl}(t)$,

$$\Omega_{nl}(t) = \left[\int_{M_1}^{M'(t)} dM n_H(M) M + \int_{M'(t)}^{M_2(t)} dM n_C(M) M \right] 6\pi G t^2 \quad (4.9)$$

where $n_H(M)$ and $n_C(M)$ respectively refer to the mass functions computed with the HDM and CDM mass formulas (3.13) and (3.14) respectively. Combining (2.1)

with (3.13) and (3.14) we obtain

$$n_C(M, t) = \nu \frac{24}{125} (\alpha\beta)^2 \frac{\mu^3}{M^4} \quad (4.10)$$

and

$$n_H(M, t) = \nu \frac{2}{15} \frac{z_{eq}}{z} \frac{\mu}{t^2} \frac{1}{M_{eq}^{2/3}} \frac{1}{M^{4/3}}. \quad (4.11)$$

As a consistency check, we note that for $M = M'(t)$ the above two expressions coincide.

By inspection of (4.8-4.11) it is clear that the integrals for $n_G(t)$ and $\Omega_{nl}(t)$ are dominated at $M = M'(t)$ and that a reasonable approximation to (4.8) will be

$$n_G(> M_1, t) \sim n_C(M', t) M' z^{-3}(t) \simeq \frac{1}{5} \nu (\alpha\beta)^2 \frac{\mu^3}{M'(t)^3} z^{-3}(t), \quad (4.12)$$

which gives

$$\begin{aligned} n_G(> M_1, t) &\sim 5\nu(\alpha\beta)^{-1/4} (G\mu)^{3/4} \left(\frac{z_{eq}}{v_{eq}}\right)^{9/4} z^{-3/4}(t) t_0^{-3} \\ &\sim 2 \cdot 10^{-4} \nu z^{-3/4}(t) h_{50}^{9/2} (h_{50}^{-1} \text{Mpc})^{-3} \end{aligned} \quad (4.13)$$

when inserting $v_{eq} = 0.1$, $G\mu = 10^{-6}$ and the values of $\alpha = 10^{-2}$ and $\beta = 10$ from Section 2. This result is plotted in Figure 1. Similarly, (4.9) can be approximated by

$$\Omega_{nl}(t) \sim n_C(M', t) M'^2 6\pi G t^2 \simeq \frac{1}{5} \nu (\alpha\beta)^2 \frac{\mu^3}{M'(t)^2} 6\pi G t^2, \quad (4.14)$$

which gives

$$\begin{aligned} \Omega_{nl}(t) &\sim \frac{15\pi}{2} \left(\frac{9}{5}\right)^{1/2} \nu (\alpha\beta)^{1/2} \left(\frac{z_{eq} G \mu}{v_{eq}}\right)^{3/2} z(t)^{-3/2} \\ &\sim 10^{-1} h_{50}^3 \nu z(t)^{-3/2} \end{aligned} \quad (4.15)$$

for the same values of the parameters as above.

At this point it looks like the cosmic string and hot dark matter model will produce too many quasar host galaxies at redshifts $z \sim 5$. However, so far loop velocities have been neglected.

Loop velocities can be taken into account by incorporating the condition (3.28). Loops which do not satisfy this criterion will not be able to accrete much mass. Note that as t_i increases, $q_x(t_i)$ remains constant whereas $\lambda_J(t_i)$ decreases. Hence, the condition (3.28) corresponds to a low mass cutoff M_c in the integrals (4.1) and (4.2). Using (3.6) and (3.26) it follows that the inequality (3.28) becomes

$$t_i z(t_i) v(t_i) < \left(\frac{6}{5}\alpha\beta\right)^{1/2} (G\mu)^{1/2} v_i^{-1/2} t_0 z(t)^{-1/2}, \quad (4.16)$$

where $v(t_i)$ is the hot dark matter velocity at time t_i and v_i is the loop velocity at the same time. After some algebra, (4.16) translates to

$$z(t_i) < \frac{6}{5}\alpha\beta G\mu z_{eq}^2 v_i^{-1} v_{eq}^{-2} z(t)^{-1} \equiv z(t_c) \quad (4.17)$$

where v_{eq} is the HDM velocity at t_{eq} . The corresponding cutoff mass is

$$M_c = M(t_c) = \frac{2}{5}\alpha\beta G\mu z(t_c)^{-1/2} z(t)^{-1} \frac{t_0}{G}. \quad (4.18)$$

It is easy to check that M_c is larger than M' , hence justifying the use of the CDM mass formula to obtain (4.18). This, however, also leads to a significant reduction in the values of $n_G(t)$ and Ω_{nl} .

The effect of loop velocities is thus to replace the estimate (4.12) by

$$n_G(> M_1, t) \sim n_C(M_c, t) M_c z^{-3}(t) \simeq 4\nu(\alpha\beta)^{1/2} (G\mu)^{3/2} v_i^{-3/2} \left(\frac{z_{eq}}{v_{eq}}\right)^3 z^{-3/2}(t) t_0^{-3}. \quad (4.19)$$

For $\alpha = \alpha_{-2} 10^{-2}$, $\beta = 10$, $v_{eq} = 0.1$ and $G\mu = (G\mu)_6 10^{-6}$, the result becomes

$$n_G(> M_1, t) \sim 4 \cdot 10^{-6} \nu z^{-3/2}(t) v_i^{-3/2} \alpha_{-2}^{1/2} (G\mu)_6^{3/2} h_{50}^6 (h_{50}^{-1} \text{Mpc})^{-3}, \quad (4.20)$$

which is also plotted in Figure 1 for $v_i = 0.25$. Similarly, (4.13) is replaced by

$$\Omega_{nl}(t) \sim n_C(M_c, t) M_c^2 6\pi G t^2 \simeq 9\pi\nu\alpha\beta(G\mu z_{eq} v_{eq}^{-1})^2 v_i^{-1} z^{-2}(t). \quad (4.21)$$

For the same parameter choices as above, this becomes

$$\Omega_{nl}(t) \sim 10^{-2} \nu \alpha_{-2} (G\mu)_6^2 v_i^{-1} z(t)^{-2} h_{50}^4. \quad (4.22)$$

Eqs. (4.20) and (4.22) are the main results of our calculations.

As a final consistency check we must verify that $M_c(t) < M_2(t)$. This is indeed true provided that

$$z(t) < \frac{3}{2} z_{eq} v_{eq}^{-1} v_i^{-1/2} \beta \alpha^{-1/2} G\mu \sim 17 h_{50}^2 \quad (4.23)$$

(for $v_i = 0.25$). However, there may be an even more restrictive condition. Since the accretion onto a moving string is not spherically symmetric, M_2 might be determined not by (4.3) but by the stronger criterion

$$q_x(t_i, t) > \alpha t_i z(t_i). \quad (4.24)$$

Using (3.26), this becomes

$$z(t_i) > \frac{5}{6} \alpha \beta^{-1} (G\mu)^{-1} v_i z(t) \equiv z_m. \quad (4.25)$$

In order for our results (4.20) and (4.22) to be valid, z_m needs to be smaller than $z(t_c)$. This will only be the case if

$$\frac{6}{5} \beta G\mu z_{eq} v_i^{-1} v_{eq}^{-1} > z(t), \quad (4.26)$$

which is marginally satisfied for $z = 4$ if $v_i = 0.25$ and $v_{eq} = 0.1$,

$$z(t) < 3 h_{50}^2. \quad (4.27)$$

For values of z larger than 4, the values of $n_G(t)$ and Ω_{nl} are suppressed beyond the results (4.20) and (4.22) since only the tail of the loop ensemble with velocities smaller than the mean velocity $v_i = 0.25$ manage to accrete a substantial amount of mass.

5. Discussion

We have studied the accretion of hot dark matter onto moving cosmic string loops and made use of the results to study early structure formation in the cosmic string plus HDM model. Our main results are expressed in Eqs. (4.20), (4.22) and (4.26).

The loop accretion mechanism is able to generate nonlinear objects which could serve as the hosts of high redshift quasars much earlier than the time cosmic string wakes start turning around (which for $G\mu = 10^{-6}$ and $v_s = 1/2$ occurs at a redshift of about 1). However, there is an upper cutoff to the redshift of large mass objects which form by this mechanism given by Eq. (4.26) and for $v_i = 0.25$ it corresponds to a redshift of about 4. For larger redshifts, only the loops with velocities sufficiently small compared to the mean loop velocity will be able to seed nonlinear objects. Note that this redshift cutoff is independent of the parameters α and ν of the cosmic string scaling distribution which must be obtained from numerical simulations and are still quite uncertain.

The fraction $\Omega_{nl}(z)$ of the total mass accreted into nonlinear objects by string loops unfortunately depends very sensitively on α and ν . On the other hand, this is not surprising since the power of the loop accretion mechanism depends on the number and initial sizes of the loops, and the scaling relation $\Omega_{nl} \sim \nu\alpha$ is what should be expected from physical considerations.

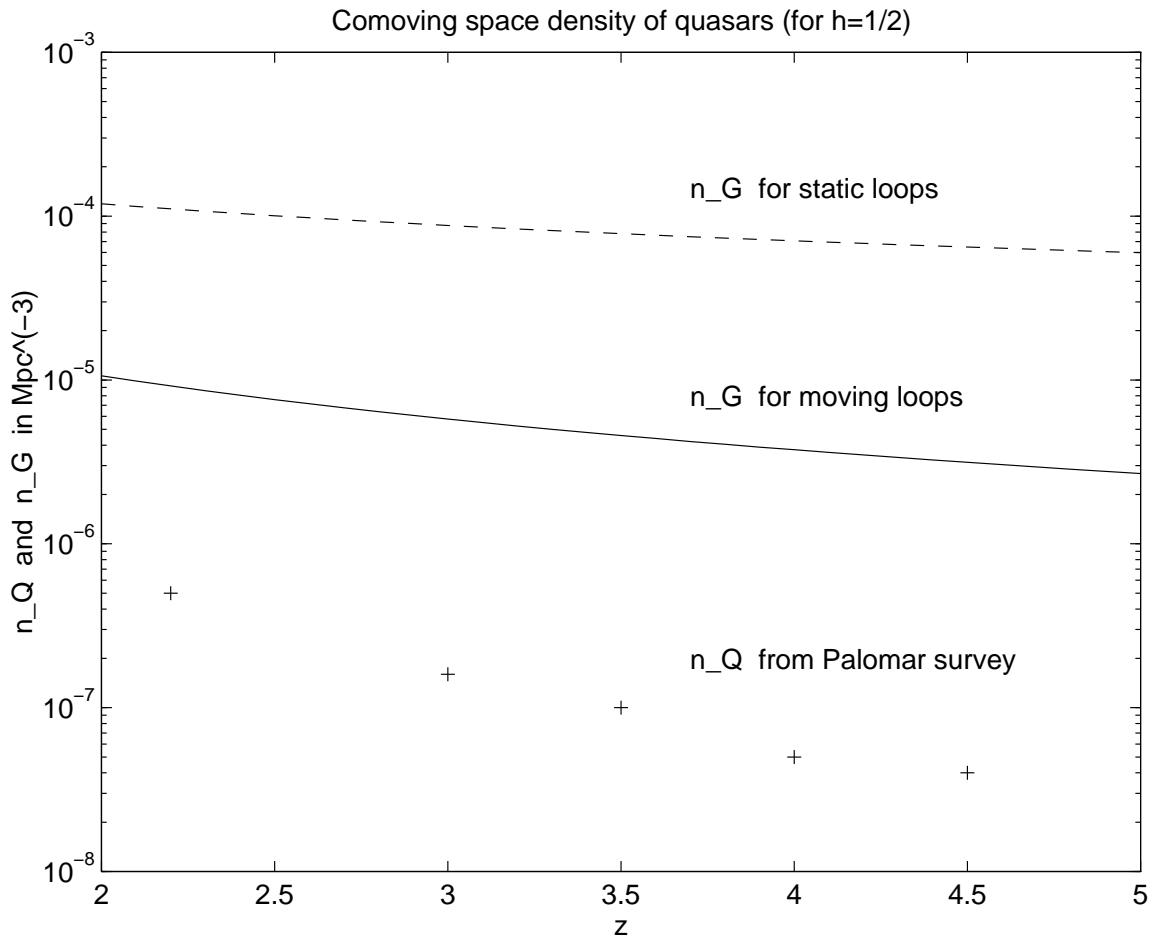


Figure 1: Comparison of the observed number density of quasars (+ marks) with the number density of proto-galaxies predicted in the cosmic string theory with hot dark matter for the parameters discussed in the text. The horizontal axis is the redshift.

For the values $\nu = 1$ and $\alpha_{-2} = 1$ which are indicated by recent cosmic string evolution simulations¹⁷⁾, we conclude from Eq. (4.20) that the loop accretion mechanism produces enough large mass proto-galaxies to explain the observed abundance of $z \leq 4$ quasars (see Figure 1). Note that the amplitude of the predicted proto-galaxy density curves depends sensitively on the parameters of the cosmic string scaling solution which are still poorly determined. Hence, the important result is that there *are* parameters for which the theory predicts a sufficient number of

protogalaxies. Since not all protogalaxies will actually host quasars, and since the string parameters are still uncertain, it would be wrong to demand that the amplitude of the n_G curve agree with that of the observed n_Q .

It is more difficult to make definite conclusions regarding the abundance of damped Lyman alpha absorption systems. In the form of Eq. (1.2), the condition for the cosmic string loop accretion mechanism to be able to explain the data is also satisfied. However, Eq. (1.2) refers to the value of Ω in baryonic matter. The corresponding constraint on the total matter collapsed in structures associated with damped Lyman alpha systems is

$$\Omega_{\text{DL}}(z < 3) > f_b^{-1} 10^{-3} \quad (5.1)$$

where f_b is the local fraction of the mass in baryons. From Eq. (4.22) it follows that the above constraint is only marginally satisfied, and this only if the local baryon fraction f_b exceeds the average value for the whole Universe of about $f_b = 0.1$. This could be another manifestation of the “baryon crisis” for galaxy clusters²⁸⁾, the fact that f_b in clusters seems to exceed what is expected based on nucleosynthesis constraints in a $\Omega = 1$ Universe. On the other hand, in the cosmic string model with HDM we expect f_b in nonlinear objects to be enhanced over the average f_b because baryons are able to cluster during the time that the HDM is prevented from accreting by the free streaming²⁹⁾. Thus, cosmic strings may be able to explain the baryon excess in clusters and restore agreement with (1.2) in a natural way. More calculations are required to resolve this issue.

In conclusion, we have established that in addition to being in agreement with large-scale structure and CMB data, the cosmic string and hot dark matter model is also able to produce a sufficient number of protogalaxies at redshifts $z \leq 4$ which could explain the observed abundance of quasars. A prediction of the model is that the distribution of these quasars should be less correlated with today’s large-scale structure than in inflation-based models, since the loops giving rise to quasars are not correlated with the long strings present at the time of equal matter and

radiation, which give the dominant contribution to today's large-scale structure. However, some correlation might still be present since the loops are correlated with the long strings from which they were split off, and since the quasar host galaxies evolve into present-day galaxies and may fall into the potential wells created by the string wakes.

Acknowledgements: We are grateful to Houjun Mo, Joel Primack, Bill Unruh, Alex Vilenkin and Simon White for useful suggestions. R. B. wishes to thank Bill Unruh and the Physics Department of the University of British Columbia for hospitality during the spring of 1995. This work is supported in part by the US Department of Energy under contract DE-FG0291ER40688, Task A (Brown) and by the Canadian NSERC under Grant 580441 (UBC).

REFERENCES

1. K. Lanzetta et al., *Ap. J. (Suppl.)* **77**, 1 (1991);
K. Lanzetta, D. Turnshek and A. Wolfe, *Ap. J. (Suppl.)* **84**, 1 (1993);
K. Lanzetta, A. Wolfe and D. Turnshek, *Ap. J.* **440**, 435 (1995);
L. Storrie-Lombardi, R. McMahon, M. Irwin and C. Hazard, 'High redshift Lyman limit and damped Lyman alpha absorbers', astro-ph/9503089, to appear in 'ESO Workshop on QSO Absorption Lines' (1995).
2. S. Warren, P. Hewett and P. Osmer, *Ap. J. (Suppl.)* **76**, 23 (1991);
M. Irwin, J. McMahon and S. Hazard, in 'The space distribution of quasars', ed. D. Crampton (ASP, San Francisco, 1991), p. 117;
M. Schmidt, D. Schneider and J. Gunn, *ibid.*, p. 109;
B. Boyle et al., *ibid.*, p. 191;
M. Schmidt, D. Schneider and J. Gunn, *Astron. J.* **110**, 68 (1995).
3. K. Subramanian and T. Padmanabhan, 'Constraints on the models for structure formation from the abundance of damped Lyman alpha systems', IUCAA preprint, astro-ph/9402006 (1994).

4. F. Briggs and A. Wolfe, *Ap. J.* **268**, 76 (1983);
K. Lanzetta and D. Bower, *Ap. J.* **371**, 48 (1992).
5. H. Mo and J. Miralda-Escudé, *Ap. J. (Lett.)* **430**, L25 (1994).
6. G. Kauffmann and S. Charlot, *Ap. J. (Lett.)* **430**, L97 (1994);
C.-P. Ma and E. Bertschinger, *Ap. J. Lett.* **434**, L5 (1994);
A. Klypin et al., *Ap. J.* **444**, 1 (1995).
7. G. Efstathiou and M. Rees, *MNRAS* **230**, 5p (1988).
8. M. Haehnelt, *MNRAS* **265**, 727 (1993).
9. J. Bond, G. Efstathiou and J. Silk, *Phys. Rev. Lett.* **45**, 1980 (1980);
G. Bisnovatyi-Kogan and I. Novikov, *Astron. Zh.* **57**, 899 (1980).
10. Ya.B. Zel'dovich, *MNRAS* **192**, 663 (1980);
A. Vilenkin, *Phys. Rev. Lett.* **46**, 1169 (1981).
11. R. Brandenberger, N. Kaiser, D. Schramm and N. Turok, *Phys. Rev. Lett.* **59**, 2371 (1987);
R. Brandenberger, N. Kaiser and N. Turok, *Phys. Rev.* **D36**, 2242 (1987).
12. A. Albrecht and A. Stebbins, *Phys. Rev. Lett.* **69**, 2615 (1992).
13. Ya.B. Zel'dovich, *Astron. Astrophys.* **5**, 84 (1970).
14. L. Perivolaropoulos, R. Brandenberger and A. Stebbins, *Phys. Rev.* **D41**, 1764 (1990);
R. Brandenberger, L. Perivolaropoulos and A. Stebbins, *Int. J. Mod. Phys.* **A5**, 1633 (1990).
15. E. Bertschinger, *Ap. J.* **316**, 489 (1987).
16. A. Vilenkin and E.P.S. Shellard, '*Cosmic strings and other topological defects*' (Cambridge Univ. Press, Cambridge, 1994);
M. Hindmarsh and T. Kibble, '*Cosmic Strings*', *Rep. Prog. Phys.* in press (1995).;
R. Brandenberger, *Int. J. Mod. Phys.* **A9**, 2117 (1994).

17. D. Bennett and F. Bouchet, *Phys. Rev. Lett.* **60**, 257 (1988);
 B. Allen and E. P. S. Shellard, *Phys. Rev. Lett.* **64**, 119 (1990);
 A. Albrecht and N. Turok, *Phys. Rev.* **D40**, 973 (1989).
18. J. Silk and A. Vilenkin, *Phys. Rev. Lett.* **53**, 1700 (1984).
19. T. Vachaspati, *Phys. Rev. Lett.* **57**, 1655 (1986);
 A. Stebbins et al., *Ap. J.* **322**, 1 (1987).
20. V. de Lapparent, M. Geller and J. Huchra, *Ap. J. (Lett.)* **302**, L1 (1986);
 M. Geller and J. Huchra, *Science* **246**, (1989);
 V. de Lapparent, M. Geller and J. Huchra, *Ap. J.* **369**, 273 (1991);
 M. Vogeley, C. Park, M. Geller, J. Huchra and R. Gott, *Ap. J.* **420**, 525 (1994).
21. N. Kaiser and A. Stebbins, *Nature* **310**, 391 (1984);
 R. Brandenberger and N. Turok, *Phys. Rev.* **D33**, 2182 (1986).
22. D. Bennett, A. Stebbins and F. Bouchet, *Ap. J. (Lett.)* **399**, L5 (1992);
 L. Perivolaropoulos, *Phys. Lett.* **B298**, 305 (1993).
23. T. Hara and S. Miyoshi, *Prog. Theor. Phys.* **81**, 1187 (1989);
 T. Hara, S. Morioka and S. Miyoshi, *Prog. Theor. Phys.* **84**, 867 (1990);
 T. Hara et al., *Ap. J.* **428**, 51 (1994).
24. D. Vollick, *Phys. Rev. D* **45**, 1884 (1992);
 T. Vachaspati and A. Vilenkin, *Phys. Rev Lett.* **67**, 1057 (1991).
25. A. Aguirre and R. Brandenberger, ‘*Accretion of hot dark matter onto slowly moving cosmic strings*’, Brown Univ. preprint BROWN-HET-995, astro-ph/9505031 (1995), *Int. J. Mod. Phys.* **D**, (in press).
26. A. Sornborger, R. Brandenberger, B. Fryxell and K. Olson, ‘*The structure of cosmic string wakes*’, Brown Univ. preprint BROWN-HET-1021 (1995).
27. R. Brandenberger and E.P.S. Shellard, *Phys. Rev.* **D40**, 2542 (1989).

28. S. White et al., *Nature* **366**, 429 (1993);
G. Steigman & J. Felten, 'The X-Ray Cluster Baryon Crisis' in *Proc. of the St. Petersburg Gamow Seminar* (1994), ed. A. Bykov & R. Chevalier; *Sp. Sci. Rev.*, in press (Dordrecht: Kluwer).
29. R. Moessner, Brown Univ. preprint, (in preparation, 1995).